

Consistent parameter fixing in the quark-meson model with vacuum fluctuations

Stefano Carignano,¹ Michael Buballa,² and Wael Elkamhawy²

¹*INFN, Laboratori Nazionali del Gran Sasso, Assergi (AQ), Italy*

²*Theoriezentrum, Institut für Kernphysik, Technische Universität Darmstadt, Germany*

We revisit the renormalization prescription for the quark-meson model in an extended mean-field approximation, where vacuum quark fluctuations are included. At a given cutoff scale the model parameters are fixed by fitting vacuum quantities, typically including the sigma-meson mass m_σ and the pion decay constant f_π . In most publications the latter is identified with the expectation value of the sigma field, while for m_σ the curvature mass is taken. When quark loops are included, this prescription is however inconsistent, and the correct identification involves the renormalized pion decay constant and the sigma pole mass. In the present article we investigate the influence of the parameter-fixing scheme on the phase structure of the model at finite temperature and chemical potential. Despite large differences between the model parameters in the two schemes, we find that in homogeneous matter the effect on the phase diagram is relatively small. For inhomogeneous phases, on the other hand, the choice of the proper renormalization prescription is crucial. In particular, we show that if renormalization effects on the pion decay constant are not considered, the model does not even present a well-defined renormalized limit when the cutoff is sent to infinity.

I. INTRODUCTION

The study of strong-interaction matter at finite density is a fascinating topic which attracts a lot of interest, both from the theory and the experimental side. While weak-coupling calculations reveal that the ground state of quantum chromodynamics (QCD) at asymptotically high baryonic chemical potentials and low temperatures is a color superconductor, the region of intermediate densities beyond nuclear matter saturation may exhibit a rich phase structure, see e.g. [1] for a review.

From a theoretical point of view, the investigation of this region is extremely challenging: due to the sign problem, ab-initio lattice simulations are unavailable at nonzero baryonic densities, so that phenomenological models are currently the main tool to access this region. A popular choice for this kind of study is the quark-meson (QM) model [2, 3], whose basic building blocks are quarks which interact with mesons. Compared to the formally similar Nambu–Jona-Lasinio (NJL) model, the QM model has the advantage of being renormalizable, a property which renders it an excellent tool for investigating the role of fluctuations in a systematic way within the framework of the functional renormalization group, e.g. [3–7].

Until a few years ago it was believed that, in the mean-field approximation, quark vacuum fluctuations could be simply left out, expecting that a redefinition of the meson potential parameters would be sufficient to take their effects into account. Such a “no-sea” or “standard mean-field approximation” (sMFA) leads however to inconsistent predictions, such as the persistence of a first-order chiral phase transition in the chiral limit at zero densities, in conflict with general expectations [8, 9]. This artifact disappears once vacuum quark fluctuations are properly taken into account [10–12], suggesting that an explicit treatment of the Dirac sea contributions is crucial.

More recently, this so-called extended mean-field approximation (eMFA) where mesonic fluctuations are still neglected has also been applied to study the effects of quark vacuum fluctuations on inhomogeneous chiral symmetry breaking phases [13]. These crystalline phases, which are characterized by the formation of a spatially modulated quark-antiquark condensate, are expected to form in cold and dense quark matter (for a recent review, see [14]). Mean-field NJL-model studies suggest that they completely cover the first-order chiral transition [15], so that the critical point (CP) is replaced by a Lifshitz point (LP), denoting the tip of the inhomogeneous island. For the QM model it was found that including the Dirac sea reduces the size of the inhomogeneous phase, but in general does not destroy it completely [13]. In particular, it was shown that the LP is at the same place as the CP of the homogeneous analysis if in vacuum the sigma-meson mass m_σ is twice the constituent quark mass, as it is always the case in the NJL model. In the QM model, however, m_σ can be chosen freely, and the inhomogeneous phase turned out to be very sensitive to this choice.

In the eMFA the diverging contribution stemming from vacuum quark fluctuations are reabsorbed by a proper redefinition of the model parameters through a fit to vacuum observables, leading to UV-finite results. As we shall see, however, this renormalization procedure must be performed with great care, as different prescriptions for the identification of the physical quantities can be employed.

In its simplest incarnation, the two-flavor QM model in the chiral limit has three free parameters, which are typically fitted in vacuum to give reasonable values of the pion decay constant f_π , the sigma meson mass m_σ and the constituent quark mass M_q . Until relatively recently, the standard procedure has been to fit the sigma meson mass to

the so-called “curvature” (or screening) mass, associated with the curvature of the QM thermodynamic potential at its minimum, while the pion decay constant is identified with the vacuum expectation value of the sigma mean-field [6, 10, 12, 16–18]. In principle, however, the physical mass of the sigma meson is given by the pole of its propagator (as recently stressed in [19, 20]), while the pion decay constant is related to the residue of the pion propagator at its pole. In light of these considerations, it was suggested in [13] to consider these “pole” quantities instead of the traditionally employed ones for the parameter fixing in the model. While in absence of Dirac sea contributions the two prescriptions become trivially equivalent, when quark loops are taken into account the sigma pole and screening masses start to differ, and the pion decay constant has to be renormalized as well.

The main objective of this work is to investigate the differences between the extended mean-field results obtained in the QM model within these two different prescriptions, with a particular emphasis on their influence on inhomogeneous chiral symmetry breaking phases. While, as we shall discuss, in the QM model homogeneous phases turn out to be relatively insensitive to the specific parameter-fixing scheme employed, for inhomogeneous phases this choice becomes crucial.

The remainder of this article is organized as follows. In Sect. II we introduce the model and give a brief summary of the basic formalism employed in [13] to study the phase diagram. After that, in Sect. III, we define two different parameter-fixing schemes and then compare the resulting phase diagrams in Sect. IV. In Sect. V we perform a Ginzburg-Landau analysis for the CP and the LP, focusing on the renormalized limit. Two further parameter-fixing schemes are briefly discussed in Sect. VI, before we draw our conclusions in Sect. VII.

II. EXTENDED MEAN-FIELD APPROACH IN THE QUARK-MESON MODEL

Before introducing the different parameter fixing prescriptions, we set the stage by reviewing the basic formalism needed for our discussion. A more detailed derivation can be found in [13].

The quark-meson model Lagrangian density is given by [2, 3]

$$\mathcal{L}_{\text{QM}} = \bar{\psi} (i\gamma^\mu \partial_\mu - g(\sigma + i\gamma_5 \vec{\tau} \cdot \vec{\pi})) \psi + \mathcal{L}_{\text{mes}} , \quad (1)$$

where ψ is a $4N_f N_c$ -dimensional quark spinor with $N_f = 2$ flavor and $N_c = 3$ color degrees of freedom, σ is the scalar field of the sigma meson and $\vec{\pi}$ the pseudo-scalar fields of the pion triplet. The purely mesonic term \mathcal{L}_{mes} contains a kinetic and a potential term,

$$\mathcal{L}_{\text{mes}} = \frac{1}{2} (\partial_\mu \sigma \partial^\mu \sigma + \partial_\mu \vec{\pi} \partial^\mu \vec{\pi}) - U(\sigma, \vec{\pi}) \quad (2)$$

with

$$U(\sigma, \vec{\pi}) = \frac{\lambda}{4} (\sigma^2 + \vec{\pi}^2 - v^2)^2 - c\sigma . \quad (3)$$

In the following we will work in the chiral limit by considering $c = 0$. The meson potential $U(\sigma, \vec{\pi})$ has then an exact $O(4)$ -symmetry, which is isomorphic to the $SU(2)_L \times SU(2)_R$ chiral symmetry, and the Lagrangian is characterized by three model parameters, g , λ and v^2 .

The thermodynamic properties of the model are encoded in the grand potential Ω . In mean-field approximation we treat the meson fields σ and π^a as classical and replace them by their expectation values [2, 3], which we assume to be static. Using standard techniques, the thermodynamic potential can then be written as the sum of a quark loop contribution Ω_q and a pure mesonic term Ω_{mes} . In particular, after combining the mesonic mean fields with the Yukawa coupling g (as detailed below for two specific examples) one finds that the quark contribution has the same form as in the NJL model, and does not depend explicitly on the QM model parameters [14].

In our discussion we will consider both the standard homogeneous case where σ is taken to be spatially constant and $\pi^a = 0$, as well as the case where the meson mean-fields are inhomogeneous. In the former it is convenient to define $\Delta = g\sigma$, which can be interpreted as a constituent quark mass. In this case, the meson contribution to the thermodynamic potential is

$$\Omega_{\text{mes}}^{\text{hom}}(\sigma, \vec{\pi}) = U\left(\frac{\Delta}{g}, \vec{0}\right) = \frac{\lambda}{4} \left[\left(\frac{\Delta}{g}\right)^2 - v^2 \right]^2 \equiv U(\Delta) . \quad (4)$$

Since at $T = \mu = 0$ the mean-fields are expected to be homogeneous, we can employ this ansatz to calculate the vacuum thermodynamic potential, which is given by

$$\Omega^{\text{vac}}(\sigma, \vec{\pi}) = -2N_f N_c \int \frac{d^3 p}{(2\pi)^3} E_{\mathbf{p}} + U(\Delta) , \quad (5)$$

where $E_{\mathbf{p}} = \sqrt{\mathbf{p}^2 + \Delta^2}$ and the first term corresponds to the contribution due to vacuum fluctuations of quarks, which plays a crucial role in our discussion.

This quark loop integral is quartically divergent and needs to be regularized. Here we employ a Pauli-Villars (PV)-inspired scheme, which is considered appropriate for dealing both with homogeneous and inhomogeneous solutions and amounts to the replacement [21]

$$E_{\mathbf{p}} \rightarrow \sum_j c_j \sqrt{E_{\mathbf{p}}^2 + j\Lambda^2}, \quad c_j = \{1, -3, 3, -1\}, \quad (6)$$

where Λ is the PV regulator. In particular, the sMFA results are recovered for $\Lambda = 0$, while for nonzero values of Λ effects of the Dirac sea are included. It is important to recall at this point that the QM model is renormalizable. Therefore, although the thermodynamic potential always depends on the chosen value of Λ , the model results should eventually become independent of the regulator when it is sufficiently large. This aspect will be investigated when discussing the different parameter fixing prescriptions.

At the minimum, where the condition $\partial\Omega_{\text{vac}}/\partial\sigma = 0$ must hold, the nontrivial solution for the sigma field, which we will denote as σ_v , satisfies the gap equation

$$\lambda \left(\frac{M_v^2}{g^2} - v^2 \right) = g^2 L_1, \quad (7)$$

where we also defined the vacuum constituent quark mass as $M_v \equiv g\sigma_v$. L_1 is a quadratically divergent loop integral which is regularized consistently with Eq. (6), see Appendix A.

Our ansatz for spatially inhomogeneous matter will be a one-dimensional chiral density wave (CDW), which is given by [22–24] (see also [14] for a more detailed discussion)

$$\sigma(z) = \frac{\Delta}{g} \cos(2iqz), \quad \pi^3(z) = \frac{\Delta}{g} \sin(2iqz), \quad \pi^1 = \pi^2 = 0. \quad (8)$$

With this type of inhomogeneous order parameter, the evaluation of the quark loop contributions to the thermodynamic potential becomes more involved but is still feasible. Compared to homogeneous matter, the mesonic contribution now contains an additional kinetic term,

$$\Omega_{\text{mes}}^{\text{CDW}}(\sigma, \vec{\pi}) = \frac{1}{2} \left(\frac{2q\Delta}{g} \right)^2 + U(\Delta), \quad (9)$$

and we recover the homogeneous limit for $q = 0$ (cf. also Eq. (8)). In spite of its simplicity, the CDW constitutes an excellent prototype to gauge the sensitivity of inhomogeneous phases with respect to the different parametrizations considered within the QM model, as previous studies have shown that the resulting phase structure for different types of spatial modulations is similar. In particular, it was shown that the position of the Lifshitz point and the second-order phase boundary to the restored phase are general results independent of the particular spatial dependence chosen for the mean fields [15, 21]. This can be seen within the context of a Ginzburg-Landau (GL) analysis, which provides a systematic framework to investigate the thermodynamic potential in vicinity of a second-order phase transition [15, 21, 25].

For this, we expand the thermodynamic potential in terms of a complex constituent-quark mass function, which in our case is given by $M(\mathbf{x}) = g(\sigma(\mathbf{x}) + i\pi^3(\mathbf{x}))$, and obtain

$$\Omega(T, \mu; M(\mathbf{x})) = \Omega(T, \mu; 0) + \frac{1}{V} \int d^3x \left\{ \frac{1}{2} \gamma_2 |M(\mathbf{x})|^2 + \frac{1}{4} \gamma_{4,a} |M(\mathbf{x})|^4 + \frac{1}{4} \gamma_{4,b} |\nabla M(\mathbf{x})|^2 + \dots \right\}. \quad (10)$$

Within this setup, the location of the CP is determined by the condition that the coefficients of the quadratic and quartic terms vanish, ie. $\gamma_2|_{\text{CP}} = \gamma_{4,a}|_{\text{CP}} = 0$, while at the LP the quadratic and the gradient terms are zero, $\gamma_2|_{\text{LP}} = \gamma_{4,b}|_{\text{LP}} = 0$ [15].

Given the structure of the thermodynamic potential, the GL coefficients γ_i can be split into a pure mesonic contribution α_i as well as a quark-loop one β_i , i.e., $\gamma_i = \alpha_i + \beta_i$ [13]. The mesonic coefficients α_i are easily obtained from Eq. (2), yielding [21]

$$\alpha_2 = -\frac{\lambda v^2}{g^2}, \quad \alpha_{4,a} = \frac{\lambda}{g^4}, \quad \alpha_{4,b} = \frac{2}{g^2}, \quad (11)$$

while the quark-loop terms β_i have the same structure as in the NJL model [15, 21]. They can be written as

$$\beta_2 = \beta_2^{\text{vac}} + \beta_2^{\text{med}}, \quad (12)$$

$$\beta_{4,a} = \beta_{4,b} = \beta_4^{\text{vac}} + \beta_4^{\text{med}}, \quad (13)$$

where the medium contributions contain Fermi distribution functions and are always UV-finite, while the vacuum contributions are given by

$$\beta_2^{\text{vac}} = -L_1|_{M=0}, \quad (14)$$

$$\beta_4^{\text{vac}} = -L_2(0)|_{M=0}, \quad (15)$$

with the regularized integrals L_1 and L_2 , as described in the appendix. As for the full thermodynamic potential, we note that here only the mesonic coefficients α_i depend explicitly on the QM model parameters, while the entire T and μ dependence of the coefficients lies in the quark contributions β_i^{med} . Since in the NJL model there are no mesonic terms¹ and $\beta_{4,a} = \beta_{4,b}$, there one finds that the positions of the CP and the LP coincide [15]. In [13] it was found that this is also true in the QM model if the vacuum value of the sigma meson mass is twice as big as the constituent quark mass. In Sect. IV we will discuss how this result depends on the parameter fixing schemes defined in the next section.

III. PARAMETER FIXING PRESCRIPTIONS

The three parameters of the QM model, g^2 , λ and v^2 , are determined by fitting three “observables”, the pion decay constant f_π , the constituent quark mass M_v and the sigma mass m_σ in vacuum. Admittedly, the sigma mass and in particular the constituent quark mass do not correspond to good observables in reality, but this is unimportant for our discussion. Here we assume that empirical values for these quantities exist, which then serve as input for the fitting procedure.²

The most commonly employed prescription in the literature associates the pion decay constant f_π with the vacuum expectation value of the sigma field σ_v , while m_σ is identified with the sigma curvature mass $m_{\sigma,c}$. The latter is defined through the equation

$$m_{\sigma,c}^2 \equiv \left. \frac{\partial^2 \Omega_{\text{vac}}}{\partial \sigma^2} \right|_{\sigma=\sigma_v, \vec{\pi}=0} = -2g^2 M_v^2 L_2(0) + 2\lambda \frac{M_v^2}{g^2}, \quad (16)$$

where the second equality is obtained by taking the second derivative of Eq. (5) and using the gap equation Eq. (7). This scheme, which we will refer to as “BC” (as in Bare f_π and Curvature mass), is thus defined by

$$\text{BC:} \quad \sigma_v \equiv \frac{M_v}{g} \stackrel{!}{=} f_\pi, \quad m_{\sigma,c}^2 \stackrel{!}{=} m_\sigma^2. \quad (17)$$

From the first equation one trivially obtains an expression for g

$$g^2 = \frac{M_v^2}{f_\pi^2}, \quad (18)$$

which can then be inserted into Eq. (16), so that we get

$$\lambda = \frac{m_\sigma^2 f_\pi^2 + 2M_v^4 L_2(0)}{2f_\pi^4}. \quad (19)$$

Finally, we use the gap equation (7) to solve for v^2 as function of the other two parameters:

$$v^2 = \frac{M_v^2}{g^2} - \frac{g^2 L_1}{\lambda}. \quad (20)$$

¹ Instead there is an additional condensate term in the NJL model, which however only contributes to γ_2 .

² For the sake of clarity, we specify that in the following f_π and m_σ always refer to the input numbers, while we will use different names for the model expressions which are identified with these quantities.

While the BC prescription is consistent in the sMFA, this is no longer the case once vacuum quark fluctuations are present. Since the latter correspond to loop corrections to the gap equation, one has to consider such corrections to the mesons as well. The resulting dressed meson propagators then take the form

$$D_j(q^2) = \frac{1}{q^2 - m_{j,t}^2 + g^2 \Pi_j(q^2) + i\epsilon}, \quad (21)$$

where $j = \sigma, \pi$ denotes the meson channel, $m_{j,t}$ is the corresponding tree-level mass, and $\Pi_j(q^2)$ describes the $q\bar{q}$ polarization function in this channel. In the vicinity of the pole this can be written as

$$D_j(q^2) = \frac{Z_j}{q^2 - m_{j,p}^2 + i\epsilon} + \text{regular terms}, \quad (22)$$

with the pole mass $m_{j,p}$ implicitly defined by $D_j^{-1}(m_{j,p}) = 0$ and the wave-function renormalization constant $Z_j^{-1} = 1 + g^2(d\Pi_j/dq^2)|_{q^2=m_{j,p}^2}$.

In contrast to the curvature mass, the pole mass corresponds to an observable quantity and should therefore be used in the renormalization procedure. For the sigma meson one finds [13]

$$D_\sigma^{-1}(m_{\sigma,p}^2) = m_{\sigma,p}^2 - \frac{1}{2}g^2(m_{\sigma,p}^2 - 4M_v^2)L_2(m_{\sigma,p}^2) - 2\lambda\frac{M_v^2}{g^2} = 0, \quad (23)$$

from which $m_{\sigma,p}$ can be determined.³ In the sMFA we have $L_2 = 0$, and hence $m_{\sigma,p} = m_{\sigma,c}$, cf. Eq. (16). In general, however, pole and curvature masses are different.

In the pion channel, on the other hand, one finds $m_{\pi,p} = m_{\pi,c} = 0$, i.e., both prescriptions are consistent with the Goldstone theorem. Nevertheless, as a consequence of the loop corrections, one gets $Z_\pi \neq 1$, which leads to a renormalization of the pion decay constant. One obtains⁴ [13]

$$f_{\pi,\text{ren}}^2 = \frac{\sigma_v^2}{Z_\pi} = \frac{M_v^2}{g^2} \left(1 - \frac{1}{2}g^2 L_2(0) \right), \quad (24)$$

which can then be identified with the physical value f_π^2 .

The prescription proposed in [13], which employs these quantities and which we will refer to as RP scheme (as in Renormalized f_π and Pole mass) is therefore defined as

$$\text{RP:} \quad f_{\pi,\text{ren}}^2 \stackrel{!}{=} f_\pi^2, \quad m_{\sigma,p}^2 \stackrel{!}{=} m_\sigma^2. \quad (25)$$

Using Eqs. (24) and (23), this yields

$$g^2 = \frac{M_v^2}{f_\pi^2 + \frac{1}{2}M_v^2 L_2(0)} \quad (26)$$

and

$$\lambda = 2g^2 \frac{m_\sigma^2}{4M_v^2} \left[1 - \frac{1}{2}g^2 \left(1 - \frac{4M_v^2}{m_\sigma^2} \right) L_2(m_\sigma^2) \right], \quad (27)$$

while v^2 is again obtained from the gap equation (7) (cf. Eq. (20)).

IV. COMPARISON OF THE SCHEMES

By a quick comparison of Eqs. (18) and (19) with (26) and (27) one immediately sees that the behavior of the model parameters as a function of the regulator is dramatically different in the two prescriptions. For instance, g^2 is

³ Special care must be taken for $m_{\sigma,p} > 2M_v$ since L_2 gets a nonvanishing imaginary part due to the open $\sigma \rightarrow q\bar{q}$ decay channel in the model. In this case we define $m_{\sigma,p}$ via the real part of L_2 , but our main conclusions will not depend on this definition.

⁴ Most easily, this can be motivated by the Goldberger-Treiman relation $M_v = g_{\text{ren}} f_{\pi,\text{ren}}$ where $g_{\text{ren}} = g\sqrt{Z_\pi}$ is the renormalized quark-pion coupling [13]. More rigorously, the pion decay constant is obtained from the pion-to-vacuum matrix element after coupling the model to an axial gauge field. From this it follows that the decay constant is directly related to the pion wave function and must be renormalized accordingly.

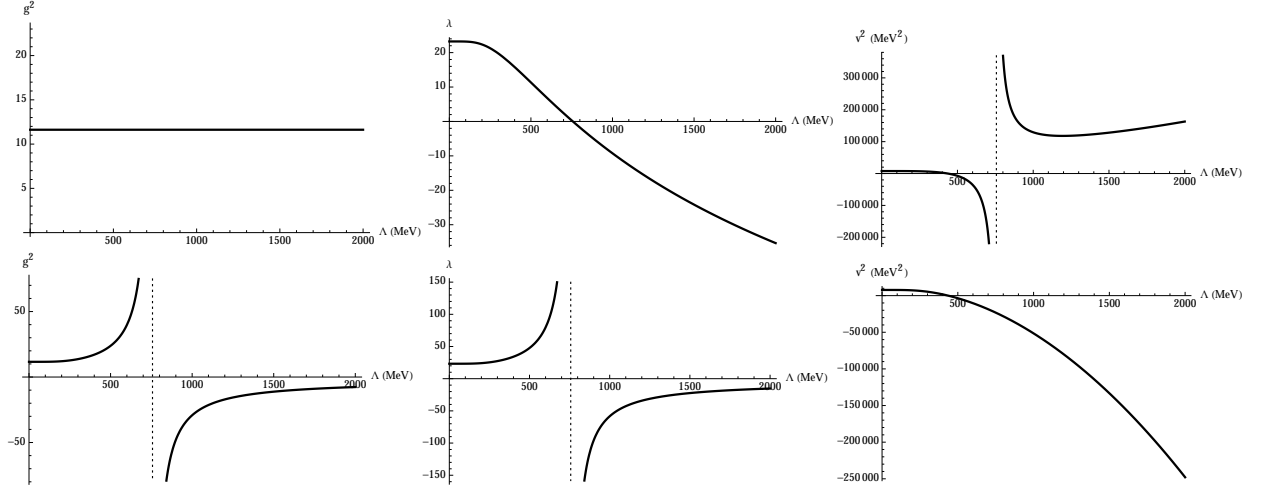


FIG. 1. Top row: g^2 , λ and v^2 as functions of the PV cutoff parameter Λ calculated within the BC scheme. Bottom: The same parameters in the RP scheme.

Λ -independent in the BC scheme, while it strongly varies with it in the RP scheme, even exhibiting a pole structure [13]. Similarly, the behaviors of λ and v^2 are entirely different. This is illustrated in Fig. 1, where, as in all our numerical examples, we have chosen the chiral limit value of the pion decay constant $f_\pi = 88$ MeV and a vacuum constituent quark mass of $M_v = 300$ MeV. For the sigma mass we took the input value $m_\sigma = 600$ MeV in this figure.

In spite of these qualitative differences, the two prescriptions yield similar results for the phase diagram if only spatially homogeneous mesonic fields are considered. In order to see this, we start from the thermodynamic potential $\Omega_{\text{hom}}(T, \mu; \Delta)$ and recall that only the meson contribution, Eq. (4), depends explicitly on the model parameters. Hence, all differences between the thermodynamic potentials in the BC and RP prescriptions will stem from this term.

As a first step, using the gap equation we substitute the parameter v^2 , which in both schemes is given by Eq. (20). Inserting this into Eq. (4) we get

$$U(\Delta) = \frac{\lambda}{4g^4} (\Delta^2 - M_v^2)^2 + \frac{1}{2} (\Delta^2 - M_v^2) L_1 + \frac{g^4}{4\lambda} L_1^2. \quad (28)$$

From this, one can clearly see that the model parameters enter U only via the ratio λ/g^4 , which will therefore be the focus of our discussion. In the BC scheme we find (cf. Eqs. (18) and (19))

$$\left(\frac{\lambda}{g^4} \right)_{\text{BC}} = \frac{m_\sigma^2 f_\pi^2 + 2M_v^4 L_2(0)}{2M_v^4}, \quad (29)$$

while for the RP scheme this ratio can be expressed as

$$\left(\frac{\lambda}{g^4} \right)_{\text{RP}} = \left(\frac{\lambda}{g^4} \right)_{\text{BC}} + \eta(m_\sigma^2), \quad (30)$$

with

$$\eta(m_\sigma^2) = \left(\frac{m_\sigma^2}{4M_v^2} - 1 \right) \delta L_2(m_\sigma^2), \quad (31)$$

where $\delta L_2(m_\sigma) = L_2(m_\sigma^2) - L_2(0)$ is a UV-finite quantity, see Appendix A. If $m_\sigma = 2M_v$ it is immediate to see that η vanishes and therefore the two expressions for λ/g^4 become identical. This result is quite remarkable, as it means that in this case both schemes yield the same homogeneous phase diagrams, despite the very different behavior of the model parameters.

In the more general case $m_\sigma \neq 2M_v$ on the other hand the two differ, so the resulting homogeneous phase diagrams will depend on the scheme of parameter fixing. In order to check this expectation, as well as determine the magnitude of this difference, we plot in Fig. 2 the phase diagrams for three different values of m_σ . While in the central panel,

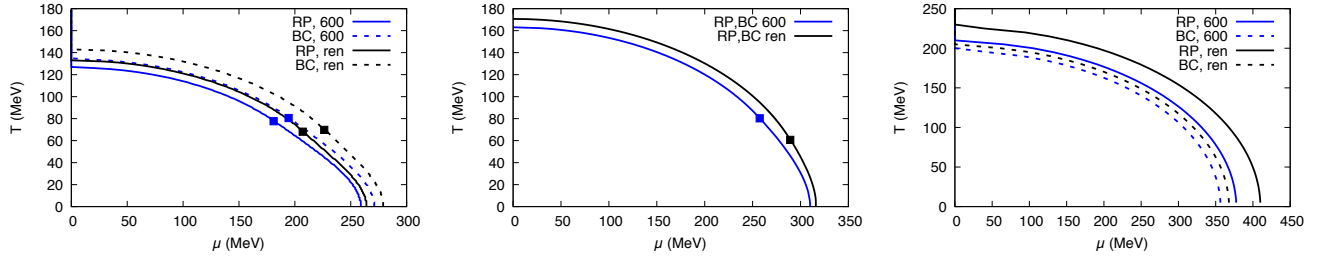


FIG. 2. Homogeneous phase diagrams for $m_\sigma = 400$ MeV (left), 600 MeV (center) and 800 MeV (right) in the two schemes. Squares denote the CP. Note the different scales! There is no CP for $m_\sigma = 800$ MeV.

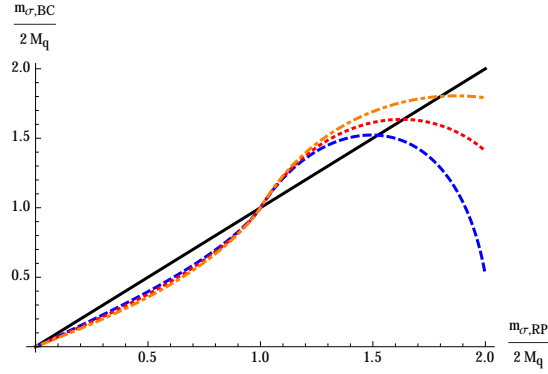


FIG. 3. Value of the sigma mass in the BC scheme which yields the same thermodynamic potential as the corresponding sigma mass in the RP scheme. The different curves correspond to different cutoff values: $\Lambda = 0$ (black solid line), $\Lambda = 700$ MeV (blue dashed line), $\Lambda = 1$ GeV (red dotted line) and the renormalized result (orange dash-dotted line).

where $m_\sigma = 2M_v$, the curves obtained in the two schemes lie on top of each other, in the other cases, the two parameter fixing prescriptions lead to different results.

The differences are however relatively small. In fact, it is possible to compensate for the change of the parameter fixing scheme by a moderate adjustment of the input sigma mass. To see this, we fix the value of f_π and the cutoff Λ , then go back to Eqs. (29) and (30) and ask for which input $m_\sigma = m_{\sigma,BC}$ in the BC scheme the ratio λ/g^4 (and hence the homogeneous phase diagram) becomes equal to the one obtained with $m_\sigma = m_{\sigma,RP}$ in the RP scheme. We arrive at the relation

$$m_{\sigma,BC}^2 = m_{\sigma,RP}^2 - \frac{2M_v^4}{f_\pi^2} \eta(m_{\sigma,RP}^2) \quad (32)$$

which is illustrated in Fig. 3 for different values of Λ . The black solid line corresponds to the result in the sMFA, where $\Lambda = 0$ and the two schemes (and consequently the two input masses) are identical. For a non-zero cutoff instead, $m_{\sigma,BC}$ is in general different from $m_{\sigma,RP}$, but there are still three points where the curves cross the black solid line, meaning that the two masses agree. These crossing points correspond to the values of the sigma mass where $\eta(m_\sigma^2) = 0$, cf. Eq. (31). In particular, as we have discussed above, this is always the case at $m_\sigma = 2M_v$. In addition, $\delta L_2(m_\sigma)$ vanishes at $m_\sigma = 0$, as well as at some higher value of m_σ , which depends on the cutoff.⁵ As a consequence, $m_{\sigma,BC}$ is always relatively close $m_{\sigma,RP}$, at least for reasonable values of the sigma mass. Recalling that the latter is not well constrained by experiments, this means that for homogeneous matter the analysis in the theoretically inconsistent BC scheme incidentally leads to results which are in practice indistinguishable from those of the correct treatment within the RP approach.

The situation is however dramatically different for inhomogeneous phases, as we will now show for the CDW solutions. Again, just like in the homogeneous case, only the meson contribution Ω_{mes}^{CDW} to the thermodynamic potential depends explicitly on the parameters, but the essential difference here is the presence of the additional

⁵ In the renormalized limit, $\Lambda \rightarrow \infty$, the value of $r = \frac{m_{\sigma,RP}}{2M_v}$ at the third crossing point is implicitly given by the equation $r = \cosh(\frac{r}{\sqrt{r^2-1}})$, which yields $r \approx 1.81$.

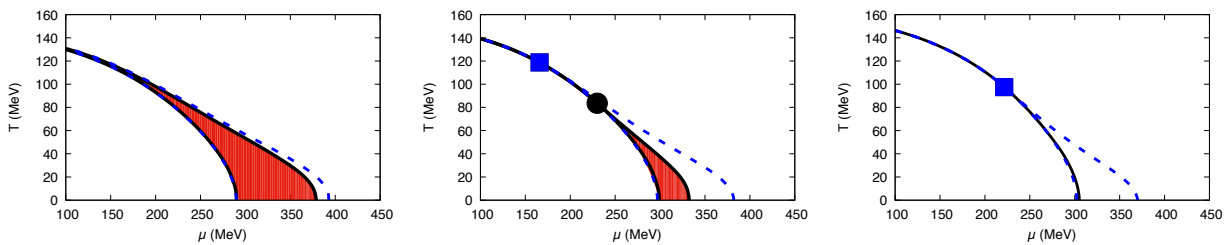


FIG. 4. Phase diagram for $m_\sigma = 2M_v$ and $\Lambda = 200$ MeV (left), 300 MeV (center) and 400 MeV (right). The shaded regions correspond to the inhomogeneous phases in the BC scheme, the blue dashed lines indicate the boundaries of the inhomogeneous phase in the RP scheme. Squares denote the critical points, which are identical in both schemes and which in the RP scheme coincide with the Lifshitz points. The dot indicates the Lifshitz point in the BC method.

kinetic term in Eq. (9). This term only contains the parameter g , which varies between different schemes, and unlike for the case of homogeneous matter no other parameter can compensate for it. We thus conclude that inhomogeneous phases are sensitive to the way of parameter fixing, even in the case $m_\sigma = 2M_v$, where the homogeneous results are the same in both schemes. In particular, while it was found that in the RP scheme the inhomogeneous phase survives in the renormalized limit [13], in the BC scheme it quickly disappears as Λ is increased.

This can be seen in Fig. 4 where the phase diagram for $m_\sigma = 2M_v$ is shown for three relatively small values of the cutoff. When $m_\sigma = 2M_v$ the homogeneous phase diagrams are identical in both schemes, so that the positions of the corresponding CPs (marked by the blue square) are the same. Furthermore, in this limit it was found that within the RP scheme the LP coincides with the CP [13]. Consequently, the inhomogeneous phase (whose boundaries are indicated by the dashed lines) extends up to that point and is only mildly affected by the increase of the cutoff. In the BC scheme, on the other hand, the LP (black circle) splits from the CP and moves towards the chemical-potential axis when Λ is increased. As a consequence, the inhomogeneous phase (shaded area) shrinks quickly, and already at $\Lambda = 400$ MeV it has disappeared completely. This behavior can be traced back to the fact that in the BC scheme, where the curvature mass $m_{\sigma,c}$ is kept fixed, the pole mass $m_{\sigma,p}$ decreases with increasing Λ . The observed shrinking of the inhomogeneous phase is then consistent with the results of Ref. [13], where it was found that in the RP scheme the size of the inhomogeneous region decreases quickly when value of $m_{\sigma,p}$ is decreased.

V. GINZBURG-LANDAU ANALYSIS FOR THE RENORMALIZED LIMIT

It is worthwhile at this point to investigate the “renormalized” behavior of the model, i.e., the limit in which the regulator Λ is sent to infinity, in the two different prescriptions. Rather than presenting a numerical analysis of the full thermodynamic potential, we will focus on the GL coefficients, for which simple analytical expressions can be obtained in the renormalized limit. In particular, we will investigate the stability of the position of the CP and the LP as the cutoff increases, and the differences between the two schemes.

The relevant coefficients associated with the position of the chiral critical point are γ_2 and $\gamma_{4,a}$, cf. Sec. II. Using again the gap equation Eq. (20), we can rewrite the mesonic α_2 contribution as

$$\alpha_2 = -\frac{\lambda}{g^4} M_v^2 + L_1, \quad (33)$$

and thus find, consistently with the discussion in the previous section for homogeneous phases, that α_2 and $\alpha_{4,a}$ (Eq. (11)) depend only on the ratio $\frac{\lambda}{g^4}$. It is then straightforward to see that the difference between the two parameter fixing prescriptions for both γ_2 and $\gamma_{4,a}$ is proportional to the difference η between these ratios, see Eqs. (30) and (31), which is a UV-finite quantity. More specifically, one finds

$$\gamma_2^{\text{RP}} - \gamma_2^{\text{BC}} = -M_v^2 \eta(m_\sigma^2), \quad (34)$$

$$\gamma_{4,a}^{\text{RP}} - \gamma_{4,a}^{\text{BC}} = \eta(m_\sigma^2). \quad (35)$$

Having determined the differences between the coefficients for an arbitrary Λ , we now calculate their renormalized

limit. For this, we focus on the BC scheme and using Eqs. (15), (29) we obtain for γ_2

$$\begin{aligned}\gamma_2^{\text{BC}} &= -\frac{f_\pi^2 m_\sigma^2}{2M_v^2} - L_2(0)M_v^2 + L_1 - L_1|_{M=0} + \beta_2^{\text{med}} \\ &\xrightarrow{\Lambda \rightarrow \infty} -\frac{f_\pi^2 m_\sigma^2}{2M_v^2} - \frac{N_f N_c}{4\pi^2} M_v^2 + \beta_2^{\text{med}},\end{aligned}\quad (36)$$

where the quadratic divergences cancel among the L_1 integrals, while the L_2 integral takes care of the remaining logarithmic terms, so that γ_2 is always UV-finite. Similarly, for the $\gamma_{4,a}$ coefficient one has

$$\begin{aligned}\gamma_{4,a}^{\text{BC}} &= \frac{f_\pi^2 m_\sigma^2}{2M_v^4} + L_2(0) - L_2(0)|_{M=0} + \beta_4^{\text{med}} \\ &\xrightarrow{\Lambda \rightarrow \infty} \frac{f_\pi^2 m_\sigma^2}{2M_v^4} + \frac{N_f N_c}{4\pi^2} \log \frac{M_v^2}{\epsilon^2} + \beta_4^{\text{med}},\end{aligned}\quad (37)$$

where in the same way as before the logarithmic divergences in the UV cancel out between the L_2 integrals. Since $L_2(0)|_{M=0}$ has an additional logarithmic divergence in the IR, we intermediately introduced a small regulator mass ϵ . This divergence is in any case cancelled by the medium contribution β_4^{med} , so that after combining these two terms the limit $\epsilon \rightarrow 0$ can be taken numerically. From these results, the renormalized limit for the coefficients in the RP prescription can now straightforwardly be obtained using Eq. (35).

Once again, the situation changes drastically when considering inhomogeneous phases. There the relevant GL coefficient $\alpha_{4,b}$ (see Eq. (11)) carries a dependence on the parameter g only, which has a completely different behavior in the two schemes. Combining it with the fermionic part, one has

$$\gamma_{4,b} = \frac{2}{g^2} - L_2(0)|_{M=0} + \beta_4^{\text{med}}, \quad (38)$$

so that in order to obtain a UV-finite result, the first term on the right-hand side must compensate the logarithmic divergence in $L_2(0)|_{M=0}$. This is the case for the RP scheme, where one obtains from Eq. (26)

$$\begin{aligned}\gamma_{4,b}^{\text{RP}} &= 2\frac{f_\pi^2}{M_v^2} + L_2(0) - L_2(0)|_{M=0} + \beta_4^{\text{med}} \\ &\xrightarrow{\Lambda \rightarrow \infty} 2\frac{f_\pi^2}{M_v^2} + \frac{N_f N_c}{4\pi^2} \log \frac{M_v^2}{\epsilon^2} + \beta_4^{\text{med}},\end{aligned}\quad (39)$$

which is again UV-finite (and for $m_\sigma = 2M_v$ coincides with $\gamma_{4,a}^{\text{RP}}$ [13] and $\gamma_{4,a}^{\text{BC}}$).

On the other hand, in the BC scheme g^2 is simply a constant, cf. Eq. (18), so that there is no additional term available to cancel the UV divergence in $L_2(0)|_{M=0}$, and the $\gamma_{4,b}$ coefficient diverges logarithmically with Λ . Recalling that $\gamma_{4,b}$ is proportional to the coefficient of the q^2 term in the GL expansion of the thermodynamic potential, cf. Eq. (10),⁶ we thus conclude that a renormalized limit of Ω does not exist, and hence the BC scheme is completely inadequate for dealing with inhomogeneous phases.

VI. OTHER PARAMETER FIXING SCHEMES

Until now, we focused our discussion on the two most commonly employed parameter fixing schemes discussed in the literature. Since the two differ in both the identification of the sigma mass and the pion decay constant, one might at this point think of introducing “hybrid” schemes which mix the prescriptions employed in the two schemes discussed.

A first possibility would be to identify f_π with the vacuum sigma expectation value as in the BC scheme, but associate m_σ with its pole value. The corresponding equations for the parameters g and λ in this “BP” scheme are

$$g^2 = \frac{M_v^2}{f_\pi^2} \quad (40)$$

⁶ Since $L_2(0)$ is negative, gradient terms become strongly disfavored at large cutoff values, which is consistent with the disappearance of the inhomogeneous phase seen in Fig. 4.

and

$$\begin{aligned}\lambda &= g^4 \left[\frac{m_\sigma^2}{2M_v^2 g^2} + \left(1 - \frac{m_\sigma^2}{4M_v^2} \right) L_2(m_\sigma^2) \right] \\ &= \frac{M_v^4}{f_\pi^4} \left[\frac{m_\sigma^2 f_\pi^2}{2M_v^4} + \left(1 - \frac{m_\sigma^2}{4M_v^2} \right) L_2(0) - \eta(m_\sigma^2) \right],\end{aligned}\quad (41)$$

from which v can again be obtained via the gap equation, cf. Eq. (20).

By a quick inspection of these expressions we see immediately that for the case $m_\sigma = 2M_v$ one has $\lambda/g^4 = 2/g^2$, so that, according to Eq. (11), $\alpha_{4,a}^{\text{BP}}$ agrees with $\alpha_{4,b}^{\text{BP}}$ and thus the CP coincides with the LP, just like in the RP scheme.⁷ The UV behavior of the GL coefficients is however very different. Focusing for simplicity on γ_2 , using Eq. (11) and comparing the result with Eq. (36) we find

$$\gamma_2^{\text{BP}} = \gamma_2^{\text{BC}} + M_v^2 \eta(m_\sigma^2) + \frac{m_\sigma^2}{4} L_2(0), \quad (42)$$

where the first two terms on the right-hand side are finite. The last term however diverges logarithmically when the cutoff is sent to infinity, and therefore γ_2^{BP} diverges as well. According to Eq. (10) and since $L_2(0)$ is negative, this means that $M = 0$ corresponds to a maximum of the thermodynamic potential, so that for $\Lambda \rightarrow \infty$ chiral symmetry never gets restored, even at arbitrarily high temperatures or chemical potentials.

The other possible hybrid scheme one can consider involves fixing the pion decay constant to its renormalized value as in the RP scheme, but identifying the sigma curvature mass with its physical value. This “RC” scheme gives

$$g^2 = \frac{M_v^2}{f_\pi^2 + \frac{1}{2} M_v^2 L_2(0)} \quad (43)$$

and

$$\begin{aligned}\lambda &= g^4 \left[\frac{m_\sigma^2}{2M_v^2 g^2} + L_2(0) \right] \\ &= \left(\frac{M_v^2}{f_\pi^2 + \frac{1}{2} M_v^2 L_2(0)} \right)^2 \left[\frac{m_\sigma^2}{2M_v^4} \left(f_\pi^2 + \frac{1}{2} M_v^2 L_2(0) \right) + L_2(0) \right].\end{aligned}\quad (44)$$

For the GL coefficient γ_2 one obtains

$$\gamma_2^{\text{RC}} = \gamma_2^{\text{BC}} - \frac{m_\sigma^2}{4} L_2(0), \quad (45)$$

which again has a logarithmic divergence in the same form as in the BP scheme, but with opposite sign. As a consequence, $M = 0$ corresponds to a local minimum of the thermodynamic potential at large cutoff values. At the same time, at large Λ the vacuum solution $M = M_v$ of the gap equation corresponds to a maximum at large Λ , so that beyond a critical cutoff value in this scheme chiral symmetry is never broken, even in vacuum.

We thus conclude that neither of these hybrid schemes is appropriate for the study of the QM model in the eMFA, not even when the analysis is restricted to homogeneous phases.

VII. CONCLUSIONS

In this work we investigated the sensitivity of the chiral phase structure of the quark-meson model, with a particular emphasis on inhomogeneous phases, to the parameter fixing prescription in an extended mean-field approximation where fermionic vacuum fluctuations are taken into account. In the most commonly employed prescription, which we referred to as BC scheme, the pion decay constant and the sigma-meson mass are identified with the vacuum expectation value of the sigma field and the curvature mass, respectively. While correct in the standard mean-field approximation, where fermionic vacuum fluctuations are neglected, this prescription is however inconsistent in the extended mean-field approximation. This is due to the fact that the quark loops not only change the ground-state of

⁷ In fact, this is consistent with the finding of [13] that for $m_{\sigma,p} = 2M_v$ the two points agree, irrespective of the choice of f_π .

the model, but also give rise to a renormalization of the meson masses and wave functions. The proper procedure, which we termed RP scheme, therefore involves the renormalized pion decay constant and the sigma pole mass.

Although these two parameter fixing schemes lead to very different behaviors of the model parameters g^2 , λ and v^2 as functions of the regulator, we found that this has only a relatively small effect on homogeneous phases: In this case, the thermodynamic potential depends only on the ratio λ/g^4 , for which the differences between the individual couplings in the two schemes cancel each other to a large extent. In particular for $m_\sigma = 2M_v$, i.e., if the sigma mass is chosen to be equal to twice the constituent quark mass in vacuum, λ/g^4 is equal in both schemes, leading to exactly the same homogeneous phase diagram. For $m_\sigma \neq 2M_v$ differences exist but are still relatively small, so that equal phase diagrams can be obtained by choosing slightly different values of m_σ in the two schemes. As a consequence, since m_σ is not well constrained by experiments, the analysis of homogeneous phases in the theoretically inconsistent BC scheme incidentally leads to results which are in practice indistinguishable from those of the correct RP approach.

For inhomogeneous phases the situation is however completely different and the choice of the proper parameter fixing scheme becomes crucial. While in the RP scheme the inhomogeneous phase was found to be relatively stable when fermionic vacuum fluctuations are included [13], in the BC scheme it disappears already at rather low values of the regulator Λ . In particular, the coincidence of the CP with the LP in the case $m_\sigma = 2M_v$ is only present when the pole mass is employed in the parameter fixing.

We obtained further insights into this behavior by performing a Ginzburg-Landau analysis in the renormalized limit, where the regulator Λ is sent to infinity. We found that the coefficients γ_2 and $\gamma_{4,a}$, which determine the location of the critical point in the homogeneous phase diagram, remain finite in both schemes. On the other hand, the coefficient $\gamma_{4,b}$, which is relevant for the Lifshitz point in the inhomogeneous case, turned out to be only finite in the RP scheme, whereas it diverges in the BC scheme. Since the GL coefficients are obtained from a Taylor expansion of the thermodynamic potential, this means that in the BC scheme the model does not even have a well defined renormalized limit if inhomogeneous phases are considered. Within the same GL framework we also studied two possible “hybrid” schemes, where either the bare pion decay constant and the sigma pole mass or the renormalized f_π and the curvature mass are used. We found that in these schemes even the coefficient γ_2 becomes UV divergent, meaning that the renormalized limit does not even exist if the model is restricted to homogeneous mean fields.

We thus conclude that in the presence of quark vacuum contributions, the parameters in the QM model should be fixed according to the RP scheme, especially when dealing with inhomogeneous phases. Although our analysis was restricted to the extended mean-field approximation, where only fermionic vacuum fluctuations are taken into account, we believe that this result also applies to more advanced approximations, e.g., for calculations performed within the framework of the functional renormalization group.

Finally we recall that the sigma meson mass and in particular the constituent quark mass do not correspond to good observables in reality. It might thus be worthwhile to think of better alternatives for future applications of the model.

Appendix A: Regularized loop functions

The loop functions which often enter our calculations are

$$L_1(M) = 4iN_fN_c \int \frac{d^4p}{(2\pi)^4} \frac{1}{p^2 - M^2 + i\epsilon} = 2N_fN_c \int \frac{d^3p}{(2\pi)^3} \frac{1}{\sqrt{\mathbf{p}^2 + M^2}}, \quad (\text{A1})$$

and

$$\begin{aligned} L_2(q^2; M) &= 4iN_fN_c \int \frac{d^4p}{(2\pi)^4} \frac{1}{[(p+q)^2 - M^2 + i\epsilon][p^2 - M^2 + i\epsilon]} \\ &= 4N_fN_c \int \frac{d^3p}{(2\pi)^3} \frac{1}{\sqrt{\mathbf{p}^2 + M^2}} \frac{1}{q^2 - 4(\mathbf{p}^2 + M^2) + i\epsilon}, \end{aligned} \quad (\text{A2})$$

which can be conveniently split into $L_2(q^2) = L_2(0) + \delta L_2(q^2)$, where only the last term can develop an imaginary part. Since these quantities are related to vacuum quark loop integrals, the argument M appearing in their expressions is typically the constituent quark mass in vacuum M_v . In light of this, throughout the paper we will omit this argument by defining $L_1(M_v) \equiv L_1$ and $L_2(q^2, M_v) \equiv L_2(q^2)$, and will explicitly write when the argument is different (eg. in the expressions for the GL coefficients, where $M = 0$).

Employing Pauli-Villars regularization with three regulators we get the following explicit expressions for the loop functions [13]:

$$L_1 \rightarrow \frac{N_f N_c}{4\pi^2} \sum_{j=0}^3 c_j M_j^2 \ln M_j^2, \quad (\text{A3})$$

$$L_2(0) \rightarrow \frac{N_f N_c}{4\pi^2} \sum_{j=0}^3 c_j \ln M_j^2, \quad (\text{A4})$$

$$\text{Re } \delta L_2(q^2) \rightarrow \frac{N_f N_c}{4\pi^2} \sum_{j=0}^3 c_j \left\{ f \left(\frac{4M_j^2}{q^2} - 1 \right) - 2 \right\}, \quad (\text{A5})$$

$$\text{Im } \delta L_2(q^2) \rightarrow -\frac{N_f N_c}{4\pi} \sum_{j=0}^3 c_j \sqrt{1 - \frac{4M_j^2}{q^2}} \theta(q^2 - 4M_j^2), \quad (\text{A6})$$

with $M_j^2 = M^2 + j\Lambda^2$ and

$$f(x) = \begin{cases} 2\sqrt{x} \arctan(\frac{1}{\sqrt{x}}), & x > 0 \\ \sqrt{-x} \ln(\frac{1+\sqrt{-x}}{1-\sqrt{-x}}), & x < 0 \\ 0, & x = 0. \end{cases} \quad (\text{A7})$$

For $\Lambda \rightarrow \infty$, it is easy to see that L_1 diverges like $\sim \Lambda^2 + M^2 \log(\Lambda)$, while $L_2(0)$ has only an M -independent logarithmic $\sim \log(\Lambda)$ divergence. More specifically, one finds

$$L_1 = \frac{N_f N_c}{4\pi^2} \left[3\Lambda^2 \log\left(\frac{4}{3}\right) + M^2 \left(\log\left(\frac{8M^2}{3\Lambda^2}\right) - 1 \right) \right] + \mathcal{O}\left(\frac{1}{\Lambda^2}\right) \quad (\text{A8})$$

and

$$L_2(0) = \frac{N_f N_c}{4\pi^2} \log\left(\frac{8M^2}{3\Lambda^2}\right) + \mathcal{O}\left(\frac{1}{\Lambda^2}\right) \quad (\text{A9})$$

The δL_2 terms are instead UV-finite. In particular, for $\Lambda \rightarrow \infty$ one can see that all the regulator-dependent terms in $\text{Re } \delta L_2(q^2)$ drop, effectively reducing it to its unregularized version:

$$\text{Re } \delta L_2(q^2) \xrightarrow{\Lambda \rightarrow \infty} \frac{N_f N_c}{4\pi^2} \left\{ f \left(\frac{4M^2}{q^2} - 1 \right) - 2 \right\}. \quad (\text{A10})$$

-
- [1] K. Fukushima and T. Hatsuda, *Rept.Prog.Phys.* **74**, 014001 (2011), arXiv:1005.4814 [hep-ph].
 - [2] O. Scavenius, A. Mocsy, I. Mishustin, and D. Rischke, *Phys.Rev.* **C64**, 045202 (2001), arXiv:nucl-th/0007030 [nucl-th].
 - [3] B.-J. Schaefer and J. Wambach, *Phys.Rev.* **D75**, 085015 (2007), arXiv:hep-ph/0603256 [hep-ph].
 - [4] B.-J. Schaefer and J. Wambach, *Nucl.Phys.* **A757**, 479 (2005), arXiv:nucl-th/0403039 [nucl-th].
 - [5] V. Skokov, B. Stokic, B. Friman, and K. Redlich, *Phys. Rev.* **C82**, 015206 (2010), arXiv:1004.2665 [hep-ph].
 - [6] T. K. Herbst, J. M. Pawłowski, and B.-J. Schaefer, *Phys. Rev.* **D88**, 014007 (2013), arXiv:1302.1426 [hep-ph].
 - [7] R.-A. Tripolt, J. Braun, B. Klein, and B.-J. Schaefer, *Phys. Rev.* **D90**, 054012 (2014), arXiv:1308.0164 [hep-ph].
 - [8] R. D. Pisarski and F. Wilczek, *Phys.Rev.* **D29**, 338 (1984).
 - [9] M. A. Halasz, A. D. Jackson, R. E. Shrock, M. A. Stephanov, and J. J. M. Verbaarschot, *Phys. Rev. D* **58**, 096007 (1998).
 - [10] V. Skokov, B. Friman, E. Nakano, K. Redlich, and B.-J. Schaefer, *Phys.Rev.* **D82**, 034029 (2010), arXiv:1005.3166 [hep-ph].
 - [11] B.-J. Schaefer and M. Wagner, *Phys.Rev.* **D85**, 034027 (2012), arXiv:1111.6871 [hep-ph].
 - [12] U. S. Gupta and V. K. Tiwari, *Phys.Rev.* **D85**, 014010 (2012), arXiv:1107.1312 [hep-ph].
 - [13] S. Carignano, M. Buballa, and B.-J. Schaefer, *Phys. Rev.* **D90**, 014033 (2014), arXiv:1404.0057 [hep-ph].
 - [14] M. Buballa and S. Carignano, *Prog. Part. Nucl. Phys.* **81**, 39 (2015), arXiv:1406.1367 [hep-ph].
 - [15] D. Nickel, *Phys.Rev.Lett.* **103**, 072301 (2009), arXiv:0902.1778 [hep-ph].
 - [16] S. Chatterjee and K. A. Mohan, *Phys.Rev.* **D85**, 074018 (2012), arXiv:1108.2941 [hep-ph].
 - [17] J. O. Andersen and A. Tranberg, *JHEP* **08**, 002 (2012), arXiv:1204.3360 [hep-ph].
 - [18] J. Weyrich, N. Strodthoff, and L. von Smekal, *Phys. Rev.* **C92**, 015214 (2015), arXiv:1504.02697 [nucl-th].

- [19] N. Strodthoff, B.-J. Schaefer, and L. von Smekal, *Phys.Rev.* **D85**, 074007 (2012), [arXiv:1112.5401 \[hep-ph\]](#).
- [20] K. Kamikado, N. Strodthoff, L. von Smekal, and J. Wambach, *Phys. Lett.* **B718**, 1044 (2013), [arXiv:1207.0400 \[hep-ph\]](#).
- [21] D. Nickel, *Phys.Rev.* **D80**, 074025 (2009), [arXiv:0906.5295 \[hep-ph\]](#).
- [22] F. Dautry and E. Nyman, *Nucl.Phys.* **A319**, 323 (1979).
- [23] M. Kutschera, W. Broniowski, and A. Kotlorz, *Phys. Lett.* **B237**, 159 (1990).
- [24] E. Nakano and T. Tatsumi, *Phys.Rev.* **D71**, 114006 (2005), [arXiv:hep-ph/0411350 \[hep-ph\]](#).
- [25] H. Abuki, D. Ishibashi, and K. Suzuki, *Phys.Rev.* **D85**, 074002 (2012), [arXiv:1109.1615 \[hep-ph\]](#).